

Investigation on the thermophoretic tension force induced by particle rotation

Shuangling Dong,^{1*} Bingyang Cao¹ and Ping Lin²

¹*Department of Engineering Mechanics, School of Aerospace Engineering, Tsinghua University, Beijing 100084, P. R. China*

²*Department of Mathematics, University of Dundee, Dundee DD1 4HN, UK*

Accepted 2015 January 27. Received 2015 January 27; in original form 2014 December 09

ABSTRACT

Considering the rotational movement of particles in fluid with temperature gradient, the viewpoint that particles in the fluid will experience thermophoretic tension force is proposed. The force is related to the particle motion in thermophoresis but different from the thermophoretic force. The procedure to obtain the thermophoretic tension force is introduced. In analogy with the lift force on a rotating particle in uniform fluid flow, the expression for thermophoretic tension force exerted on a particle is given under the influence of temperature gradient. It is suggested that the thermophoretic tension force is perpendicular to the rotational axis and the direction of temperature gradient. The role of thermophoretic tension force is analysed for thermophoresis in microchannel and laboratory experiment related with the evolution of protoplanetary discs.

Key words: hydrodynamics – methods: analytical – protoplanetary discs – ISM: kinematics and dynamics.

1 INTRODUCTION

Under thermal gradient, microparticles suspended in a fluid medium will be driven in a direct motion, which is called thermophoresis. When exposed to an intense beam of light, a particle will be heated unevenly. The gas surrounding the particle takes on a temperature gradient and results in the force driving the particle to move in the direction of the light, which is known as photophoresis. Searching for the evolution of protoplanetary disc and its connection to observations, it is important to investigate the interaction between dust particles and the surrounding gas. Both thermophoresis and photophoresis in the process are induced by a thermal gradient. When the net thermophoretic force exceeds the sticking force existing between particles, aggregated dust particles break up into smaller fragments (Wurm 2007). The dynamic contact processes are related with particle size and aggregation structure (Geretschauser, Speith & Kley 2011; Kataoka et al. 2013). The spatial region influenced by thermophoresis can be increased as the light source is turned off and the total thermophoretic force for many particles becomes larger (Wurm 2007). For particles with size of dozens of micrometers in protoplanetary discs, this effect becomes important when the particles move into the shadow. In the Solar system, interplanetary dust particles under the heat radiation also experience the thermophoretic motion. Thermophoresis can be used for separation of microparticles and capture of DNA and other biological macromolecules. Microscale thermophoresis has been developed to

analyse intermolecular interactions in recent years (Wienken et al. 2010), which is based on the thermophoretic movement at microscopic scale. A thermal gradient force microscope has also been developed by Aumatell & Wurm (2014) to investigate the contact mechanism of ice microparticles.

Thermophoretic movement, which is also known as Soret effect, can appear in gas, liquid and solid medium (Artola & Rousseau 2007; Barreiro et al. 2008). Generally, the particles move towards the lower temperature region; however, they may drift to the opposite hot medium for special cases (Putnam, Cahill & Wong 2007). Investigation on thermophoresis in gas is relatively more mature than that in liquid. For gas thermophoresis, the Boltzmann equation can be simplified and solved to obtain the velocity distribution and then the thermophoretic force by integrating the stress. The flow around particles is categorized into three regimes as the continuous flow, the transitional flow and the free molecular flow regime with the increase of Knudsen number. In the free molecular flow regime, it is shown that the thermophoretic velocity is independent of particle radius by numerical simulation (Waldmann 1959). When the Knudsen number tends to zero with very high thermal conductivity of a particle, negative thermophoresis may exist in the continuous flow regime (Yamamoto & Ishihara 1988). For the investigation of the transitional regime, numerical approaches have been used for solving the Boltzmann equation.

The contributing factors that affect the thermophoretic force include the thermal conductivity of particles, the temperature of the gas and the flow regime. For the free molecular flow regime, the thermophoretic force increases as the pressure increases, whereas in the continuous flow regime the opposite effect occurs. The

* E-mail: doingL@163.com

thermophoretic mobility shows almost linear increase with the temperature in a gas; however, its relation with particle size needs further investigation (Braibanti, Vigolo & Piazza 2008). One of the first investigations on thermophoretic velocity of spherical particles was performed by Epstein (1929) in the slip flow regime. When the thermal conductivity of particles is very high, Epstein's relationship underestimates the thermophoretic force. The thermophoretic force and velocity were calculated by Brock (1962) in the continuum flow regime, which also did not agree well with experimental data for particles with high conductivity. The validation of Brock's expression can be extended through the entire flow regime by adjusting the coefficients (Talbot et al. 1980). Considering the collision between particle and gas molecules, a kinetic theory based on the linearized Bhatnagar–Gross–Krook (BGK) model was proposed by Beresnev & Chernyak (1995) for thermophoresis. For complete thermal and momentum accommodation, their expression was reduced to Waldmann's equation (Waldmann 1959). By comparison of the previous models and experimental results, it was shown that the impact of the accommodation coefficient can be predicted correctly (Sagot 2013).

The particle in thermophoresis is generally considered to move along the direction of the thermal gradient and the thermophoretic force is exerted in the same direction, which may not conform to reality. The actual temperature gradient around a particle is relatively complex with different behaviour of particle motion and the impact of thermophoresis should not just exhibit in this way. In fact, rotation is one of the main features in particle motion; for instance, ice particles in protoplanetary disc will rotate along or perpendicular to the direction of temperature gradient. For the temperature distribution in the actual gas, there are various factors promoting the initial particle rotation, such as the shear effect in jet and the deviation between the centroid and body centre of a particle. The consideration that the temperature distribution around a particle is induced by a uniform gradient and there exists only thermophoretic force acting along the gradient is inadequate. Based on the above analyses, the thermophoretic tension force is proposed in the present study. When a particle rotates in fluid with temperature gradient, there exists the thermophoretic tension force acting in the direction perpendicular to the gradient.

The rest of the article is organized as follows. First, we present the expression of thermophoretic tension force in Section 2. Then, in Section 3, we show our experiment on the thermophoresis in a microchannel to validate the role of thermophoretic tension force. Previous laboratory experiment related with the evolution of protoplanetary discs is also analysed in this section. Finally, our conclusions are summarized in Section 4.

2 EXPRESSION OF THERMOPHORETIC TENSION FORCE

Consider a temperature distribution with uniform gradient, as shown in Fig. 1(a); the particle rotates in the fluid. According to the conventional approach, the expression of thermophoretic tension force can be derived by solving the Laplace equation for temperature and the Stokes equation of velocity jointly. When solving the velocity by Stokes equation, the wall boundary conditions for velocity contain rotational component, thus the distribution function of the tangential velocity near the wall is not just in the form of a sinusoidal term, which is different from the case without rotation.

As the process for solving the above equations is complicated, an analogy-based approach is adopted here to obtain the

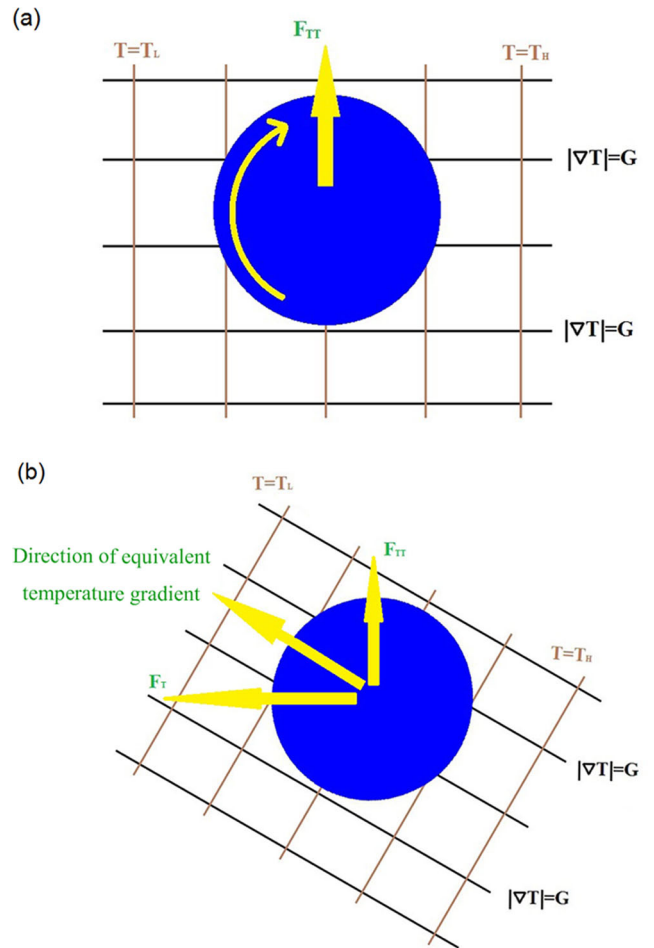


Figure 1. Spherical particles in the fluid with uniform temperature gradient. The particle is rotating in the fluid. (a) The thermophoretic tension force exerted on a rotating particle, where $|\nabla T|$ is the magnitude of temperature gradient and F_{TT} is the thermophoretic tension force. (b) The thermophoretic-related force exerted on a particle in the equivalent temperature field, where F_T represents the thermophoretic force.

expression for the thermophoretic tension force. For the thermophoretic force, the temperature equation needs to be solved first, then the velocity equation. The wall boundary conditions of velocity depend on the solution of the temperature distribution. After deriving the velocity distribution and integrating the stress, the expression for thermophoretic force is obtained. The above process is equivalent to the determination of the drag force acting on a particle when velocity boundary condition at wall for the Stokes equation is taken as thermophoretic velocity.

When calculating Magnus lift force, the wall boundary of velocity consists of two components of translation and rotation. The two fluid induced forces are orthogonal to each other. For the thermophoretic tension force, the velocity boundary at wall consists of two parts, one is contributed by temperature gradient and the other is the rotational velocity component. The temperature contribution can be replaced with the thermophoretic velocity. The thermophoretic tension force can be obtained with the translational and rotational velocity boundary components. It is consistent with the equations and boundary conditions for deriving the Magnus lift force; therefore this analogy approach is effective and can be performed.

The thermophoretic force can be expressed as

$$\mathbf{F}_{rmT} = \frac{-6\pi d_p \mu^2 C_s (K + C_t Kn)}{\rho(1 + 3C_m Kn)(1 + 2K + 2C_t Kn) T} \nabla T, \quad (1)$$

where d_p is the diameter of a particle, μ is the viscosity of the fluid, K is the ratio of thermal conductivity, ρ is the density of the fluid, T is the temperature of the fluid and Kn is the Knudsen number representing the ratio of the molecular mean-free path to the particle diameter. C_t , C_m and C_s represent the thermal exchange coefficients and the thermal slip coefficient, respectively.

The magnitude of the thermophoretic force

$$F_T = 3\pi \mu d_p U_T, \quad (2)$$

where the equivalent fluid velocity

$$U_T = \frac{2\mu C_s (K + C_t Kn)}{\rho(1 + 3C_m Kn)(1 + 2K + 2C_t Kn) T} |\nabla T| = B |\nabla T|. \quad (3)$$

When a rotating ball is moving forward in the air, its trajectory will deviate from the original direction, which is known as the Magnus effect (Magnus 1853). The spinning ball is not only influenced by gravitational force but also by the Magnus lift force due to the rotation, thus its movement shows an obvious arc trajectory. Magnus effect exists in many sports especially in ball games, such as the loop in table tennis and the banana kick in football (Mehta 1985). This effect has also been applied in design of ballistics, aircraft and stabilization for ships (Swanson 1961; Morisseau 1985; Seifert 2012).

The Magnus lift force can be determined by (Borg, Söderholm & Essén 2003)

$$\mathbf{F}_M = \frac{1}{8} C_M \rho \pi d_p^3 \boldsymbol{\omega} \times \mathbf{U}, \quad (4)$$

where $C_M = 1 + O(\text{Re})$ and $\boldsymbol{\omega}$ is the angular velocity of the particle. If the Reynolds number $\text{Re} = \frac{\rho V d_p}{\mu}$ for particle movement is small, then $C_M = 1$ in the above equation. For the particle thermophoresis with normal temperature gradient, the density of air $\rho = 1.29 \text{ kg m}^{-3}$ and the viscosity $\mu = 1.8 \times 10^{-5} \text{ Pa s}$ at room temperature, if the particle diameter $d_p = 2.0 \times 10^{-6} \text{ m}$ and the thermophoretic velocity $U_T = 5.0 \times 10^{-3} \text{ m s}^{-1}$, then $\text{Re} = 7.2 \times 10^{-4}$, which satisfies the above creep flow condition.

As the impact on a rotating particle by the surrounding gas under thermal gradient is similar to that in uniform flow, if the fluid velocity in Magnus force equation is replaced by the equivalent thermophoretic velocity, then the thermophoretic tension force can be expressed by

$$\mathbf{F}_{TT} = \frac{1}{8} \rho \pi d_p^3 \boldsymbol{\omega} \times \mathbf{U}_T. \quad (5)$$

As shown in Fig. 1(a), the direction of the thermophoretic tension force is perpendicular to the direction of temperature gradient of the surrounding gas and the rotation axis of the particle, which can also be deduced from the above equation. When the spinning axis is parallel to the direction of temperature gradient, the influence of thermophoretic tension force can be neglected, which is in agreement with the observation by van Eymeren & Wurm (2012). However, when the temperature gradient is considerably large and the rotation is moderately fast, the effect of thermophoretic tension force should be considered. For thermophoretic motion of particles with radius of μm magnitude, the ratio of F_T/F_{TT} can be about several dozens. For example, assuming the radius is $100 \mu\text{m}$ and $\omega = 2 \text{ Hz}$, the ratio becomes about 30 for particles. On the other hand,

the effect gets stronger for increased rotation with slow magnitude as to satisfy the condition for Stokes equation of gas velocity. The limitations of equation (5) are that the radius of a particle is μm magnitude and the rotation ω is not so large. The critical magnitude of the angular velocity depends on the size of the particle and the viscosity of the medium. The critical particle size is related with the Reynolds number for particle movement. Taking the particle in air for example, assuming the thermophoretic velocity $U_T = 1 \text{ mm s}^{-1}$ and the particle diameter $d_p = 300 \mu\text{m}$, then $\text{Re} = 0.0216$, which can be considered as the approximate upper limit for the flow condition with $C_M = 1$. The particle diameter should be less than $300 \mu\text{m}$ and larger than several hundred nanometers as satisfying the condition for flow equation in this case. For particle diameter $d_p = 300 \mu\text{m}$, if we define the rotational Reynolds number $\text{Re}_\omega = \frac{\rho \omega d_p^2}{2\mu}$, the upper critical angular velocity should be $\omega = 6.67$ corresponding to the above particle size, which is inversely proportional to the square of particle diameter.

In fact, the thermophoretic tension force can be interpreted more easily in the following procedure. As shown in Fig. 1(b), the fluid around is driven near the wall with the rotation of spherical particles. The corresponding temperature gradient has also been rotated and then the equivalent thermophoretic-related force changes. Thermophoretic force and thermophoretic tension force are equivalent to the two components of resultant thermophoretic force.

3 IMPACT OF THERMOPHORETIC TENSION FORCE

As a qualitative analysis with comparative experiments, the thermophoresis of particles in a microchannel has been observed for verification. The schematic diagram of the experimental setup is depicted in Fig. 2. A microfluidic device is fabricated by using stainless steel and there are three channels on the substrate sealed with an optically clear plastic film. Two larger side channels with the same length of 20 mm, width of 2.0 mm and depth of 1.5 mm are for the hot and cold water streams to generate temperature gradient. The central smaller channel for particle samples is 20 mm long, 400 μm wide and 30 μm deep. A dual-channel syringe pump was used to suck cold and hot water streams from two water baths into two respective larger channels. In order to maintain a linear temperature distribution across the sample microchannel, the counter flow

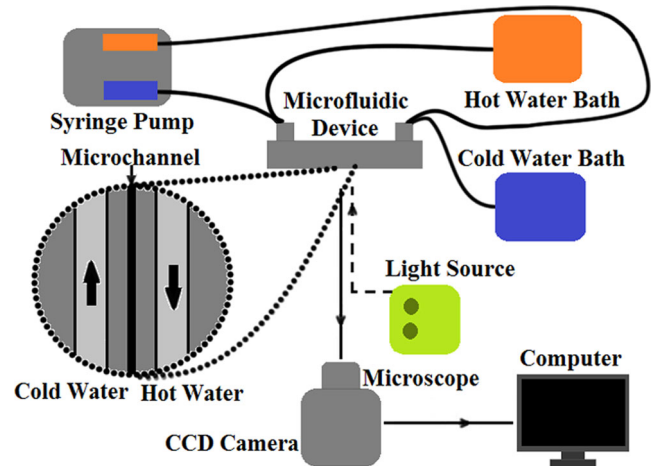


Figure 2. The experimental setup for the thermophoresis investigation. The microfluidic device consists of two larger channels for keeping temperature difference and one central sample microchannel.

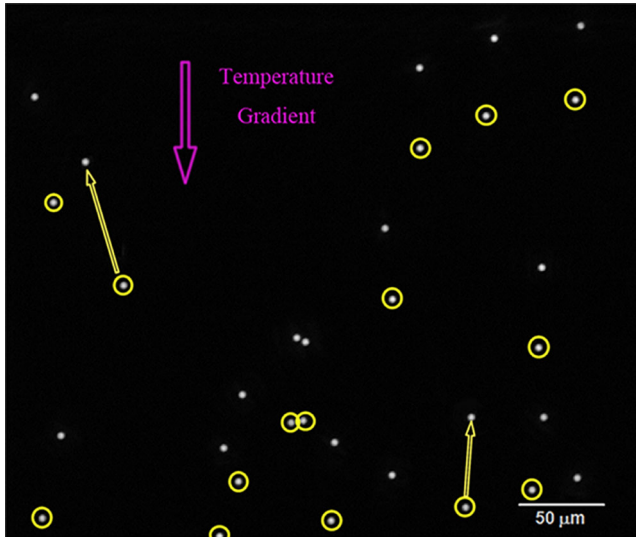


Figure 3. Particle movement in microchannel under temperature gradient.

heat transfer mode was utilized in two water channels with a sucking flow rate of $0.1 \text{ cm}^3 \text{ s}^{-1}$. The temperatures of two water baths were set to be 278 and 353 K, which ensures a nearly linear temperature change from 315 to 321 K with a gradient of about $1.5 \times 10^4 \text{ K m}^{-1}$ in the central portion of the microchannel. The dynamic thermophoretic behaviour of particles was observed with mercury lamp illumination under an inverted microscope. Sequences of images captured by a CCD camera were stored in a personal computer for further analysis.

As the sidewalls of the channel were maintained at respective constant temperatures, particles in the channel moved towards the colder side driven by the temperature gradient, which is shown in Fig. 3. Although counter flow mode ensures uniform temperature gradient and the high thermal conductivity of stainless steel helps providing a large range of background temperature, there are measurement error sources in the experiment. For instance, there existed temperature fluctuations near the side wall of the channel caused by depletion and surface roughness. Consequently, the middle portion across the channel has been selected for measurement. Due to the non-uniform distribution of the particles, some might move close to each other, such as the two particles in the central part of Fig. 3. Therefore, particles with a relatively long distance were chosen for analyses.

Through careful observation, it can be found that the particles experienced movement perpendicular to the direction of temperature gradient. There may be several possible reasons for the transversal movement. Test particles used here are spherical polystyrene (PS) particles with a diameter of $4.8 \mu\text{m}$. For this size, the Brownian movement is very small, especially when they are compared with the thermophoretic motion. Furthermore, the direction of Brownian velocity is constantly changing and it cannot induce large perpendicular movement in one direction. Therefore, the effect of Brownian motion can be eliminated. As the image plane was horizontal, the perpendicular particle movement was not influenced by the gravity, while gravitational settling showed little effect on the movement in the direction of gravity. With such small channel size, the possible natural convection effect on thermophoresis can be negligible, which has been analysed by Duhr, Arduini & Braun (2004). As the testing channel was well enclosed, the fluid in the microchannel was static on the whole and the microflow impacting on the

particle acted almost along the direction of the temperature gradient. In addition, the volume fraction of particle was around 0.02%, and the particle–particle interaction became insignificant. Although PS particles were slightly negative charged here in the water, the little influence of static charge on thermophoresis was in the direction of the temperature gradient. There was no magnetic fields in the experiment, thus magnetism showed no impact on the particle movement. The maintaining of the uniform temperature gradient was realized by heat conduction rather than the light illumination and the fluorescent technique for observation did not induce the transversal photophoretic movement. Although there existed slight fluctuation (with a maximum 3% deviation) near the two side walls of the channel, the temperature distribution was almost linear with uniform thermal gradient, especially in the central portion along the channel. Among the above possibilities, it is concluded that the rotation contributes most for the perpendicular movement. The transverse velocity of the particle is considered to be caused by the thermophoretic tension force.

Images were captured in sequence. As the temperature gradient was more uniform in the central portion of the channel, two images were chosen in the centre part both along and across the channel. The distribution of particles was relatively uniform and the particles were easily distinguishable in the two images. We have overlaid the two images in Fig. 3, where each particle at earlier time was marked with a circle. The two selected particles were highlighted with accompanied arrows. Based on the measurement, the velocity of particles was around $0.3 \mu\text{m s}^{-1}$. The particle highlighted in the left side had the maximal perpendicular velocity among the particles presented, while the velocity of the particle highlighted in the right side was of moderate magnitude. The direction of thermal gradient has been shown in the figure and the plane of the image was perpendicular to the gravity force. Particle movement was mainly horizontal with very slight vertical settlement. The maximal ratio between the sideward displacement and the principal displacement for particles was about 0.3. The ratio of F_T/F_{TT} became greater than 3. As the kinematic viscosity of the air is about 8–15 times larger than that of water and the particle size is different, the measurement was different from that discussed below equation (5) with an assumed angular velocity. Due to the particle’s spherical shape, the rotational velocity of a particle could not be observed and measured with our experimental techniques. Comparison between the experimental result and our theory was not performed quantitatively. However, an estimation of the frequency can be performed. For particle with diameter of $4.8 \mu\text{m}$, as the kinetic viscosity of water is about $6 \times 10^{-7} \text{ m}^2 \text{ s}^{-1}$ and $F_T/F_{TT} = 5000$ is needed at most to show the sideward effect, then the corresponding angular velocity ω should be 125. As the particle diameter was relatively small in the experiment and the physical behaviour is different between water and air, the deviation is much larger. Of course, effective techniques for measuring the angular velocity of a particle need to be developed in our future investigation.

Another case originates from the evolution of protoplanetary discs. By laboratory experiments, the related thermophoresis and photophoresis in these phenomena can be simulated. For photophoresis, sideward particle motion has been observed and measured. A maximum value of about 52° has been observed between force induced by photophoresis and the incident light (Loesche et al. 2014). Besides, numerical and experimental investigations by Küpper et al. (2014) also showed sideward motion clearly. For thermophoresis, particles were trapped between a Peltier element at 250 K and a tank with liquid nitrogen at 77 K (van Eymeren & Wurm 2012). The diameter of particles ranges from 20 micrometers

to several hundreds of micrometers. It can be seen obviously that the phoretic force along the direction of temperature gradient was dominant. However, particle rotation perpendicular to the temperature gradient axis and radial drift were both observed in the experiment, which coincides with the present consideration that thermophoretic tension force leads to the transversal movement.

4 CONCLUSION

Considering the rotational feature of particles in actual fluids with temperature gradient, thermophoretic tension force is proposed related with thermophoresis but unlike thermophoretic force. The solving process for obtaining the tension force is simply introduced. By using an analogy method, the expression for thermophoretic tension force has been given conveniently. Combined with the spatial transformation, the origin of the tension force has been explained. It is indicated that the thermophoretic tension force is perpendicular to the temperature gradient of the fluid and rotational axis of the particle. This has important implications for the movement of dust and ice particles in the evolution of protoplanetary disc. Experiments on thermophoresis have been performed in microchannel. The transversal movement of the particles that has been observed is considered to be caused mainly by the thermophoretic tension force. In the future study, quantitative experimental results and molecular dynamic simulations will be needed to validate the expression for the thermophoretic tension force.

ACKNOWLEDGEMENTS

We thank Professor Zengyuan Guo and Professor Chun Yang for the valuable discussion. This work is financially supported by National Natural Science Foundation of China (Nos. 51406098, 51356001, 51322603, 51136001). We also thank the China Postdoctoral Science Foundation (No. 2014M560967).

REFERENCES

- Artola P. A., Rousseau B., 2007, *Phys. Rev. Lett.*, 98, 125901
 Aumatell G., Wurm G., 2014, *MNRAS*, 437, 690
 Barreiro A., Rurali R., Hernandez E. R., Moser J., Pichler T., Forró L., Bachtold A., 2008, *Science*, 320, 775
 Beresnev S., Chernyak V., 1995, *Phys. Fluids*, 7, 1743
 Borg K. I., Söderholm L. H., Essén H., 2003, *Phys. Fluids*, 15, 736
 Braibanti M., Vigolo D., Piazza R., 2008, *Phys. Rev. Lett.*, 100, 108303
 Brock J. R., 1962, *J. Colloid. Sci.*, 17, 768
 Duhr S., Arduini S., Braun D., 2004, *Eur. Phys. J. E*, 15, 277
 Epstein P. S., 1929, *Z. für Phys.*, 54, 537
 Geretschauser R. J., Speith R., Kley W., 2011, *A&A*, 536, A104
 Kataoka A., Tanaka H., Okuzumi S., Wada K., 2013, *A&A*, 554, A4
 Küpper M., de Beule C., Wurm G., Matthews L. S., Kimery J. B., Hyde T. W., 2014, *J. Aerosol. Sci.*, 76, 126
 Loesche C., Teiser J., Wurm G., Hesse A., Friedrich J. M., Bischoff A., 2014, *ApJ*, 792, 73
 Magnus G., 1853, *Ann. Phys.*, 164, 1
 Mehta R. D., 1985, *Annu. Rev. Fluid Mech.*, 17, 151
 Morisseau K. C., 1985, *Nav. Eng. J.*, 97, 51
 Putnam S. A., Cahill D. G., Wong G. C. L., 2007, *Langmuir*, 23, 9221
 Sagot B., 2013, *J. Aerosol. Sci.*, 65, 10
 Seifert J., 2012, *Prog. Aerosp. Sci.*, 55, 17
 Swanson W. M., 1961, *Trans. ASME J. Basic Eng.*, 83, 461
 Talbot L., Cheng R. K., Schefer R. W., Willis D. R., 1980, *J. Fluid Mech.*, 101, 737
 van Eymeren J., Wurm G., 2012, *MNRAS*, 420, 18
 Waldmann L., 1959, *Z. für Naturforschung A*, 14, 589
 Wienken C. J., Baaske P., Rothbauer U., Braun D., Duhr S., 2010, *Nature Commun.*, 1, 100
 Wurm G., 2007, *MNRAS*, 380, 683
 Yamamoto K., Ishihara Y., 1988, *Phys. Fluids*, 31, 3618

This paper has been typeset from a Microsoft Word file prepared by the author.